

# Optical Identification of 15 Micron Sources in the AKARI Performance Verification Field toward the North Ecliptic Pole

Hideo MATSUHARA,<sup>1</sup> \* Takehiko WADA,<sup>1</sup> Chris P. PEARSON,<sup>1,10</sup> Shinki OYABU,<sup>1</sup>  
Myungshin IM,<sup>2</sup> Koji IMAI,<sup>1</sup> Toshinobu TAKAGI,<sup>1</sup> Eugene KANG,<sup>2</sup>  
Narae HWANG,<sup>2</sup> Woong-Seob JEONG,<sup>1</sup> Hyung Mok LEE,<sup>2</sup> Myung Gyoon LEE,<sup>2</sup>  
Soojong PAK,<sup>3</sup> Stephen SERJEANT,<sup>4</sup> Takao NAKAGAWA,<sup>1</sup> Hitoshi HANAMI,<sup>5</sup>  
Hanae INAMI,<sup>1</sup> Takashi ONAKA,<sup>6</sup> Naofumi FUJISHIRO,<sup>1†</sup> Daisuke ISHIHARA,<sup>6</sup>  
Yoshifusa ITA,<sup>1</sup> Hirokazu KATAZA,<sup>1</sup> Woojung KIM,<sup>1</sup> Toshio MATSUMOTO,<sup>1</sup>  
Hiroshi MURAKAMI,<sup>1</sup> Youichi OHYAMA,<sup>1</sup> Itsuki SAKON,<sup>6</sup> Toshihiko TANABÉ,<sup>7</sup>  
Kazunori UEMIZU,<sup>1</sup> Munetaka UENO,<sup>8</sup> and Hidenori WATARAI<sup>9</sup>

<sup>1</sup>*Institute of Space and Astronautical Science, Japan Aerospace Exploration Agency,  
Sagamihara, Kanagawa 229 8510*

<sup>2</sup>*Department of Physics & Astronomy, FPRD, Seoul National University,  
Shillim-Dong, Kwanak-Gu, Seoul 151-742, Korea*

<sup>3</sup>*Kyung Hee University, 1 Seocheon-dong, Giheung-gu, Yongin-si Gyeonggi-do 446-701, Korea*

<sup>4</sup>*Astrophysics Group, Department of Physics, The Open University, Milton Keynes, MK7 6AA, UK*

<sup>5</sup>*Iwate University, 3-18-8 Ueda, Morioka, 020-8550*

<sup>6</sup>*Department of Astronomy, School of Science, University of Tokyo, Bunkyo-ku, Tokyo 113-0033*

<sup>7</sup>*Institute of Astronomy, University of Tokyo, Mitaka, Tokyo 181-0015*

<sup>8</sup>*Department of Earth Science and Astronomy, Graduate School of Arts and Sciences,  
The University of Tokyo, Meguro-ku, Tokyo 153-8902*

<sup>9</sup>*Office of Space Applications, Japan Aerospace Exploration Agency, Tsukuba, Ibaraki 305-8505*

<sup>10</sup>*ISO Data Centre, ESA, Villafranca del Castillo, Madrid, Spain.*

(Received ; accepted )

## Abstract

We present the results of optical identifications for 257 mid-infrared sources detected with a deep 15  $\mu\text{m}$  survey over approximately 80 arcmin<sup>2</sup> area in the AKARI performance verification field near the North Ecliptic Pole. The 15  $\mu\text{m}$  fluxes of the sources range from 1 mJy down to 40  $\mu\text{Jy}$ , approximately a half of which are below 100  $\mu\text{Jy}$ . Optical counterparts were searched for within a 2-3 arcsec radius in both the  $BVRi'z'$  catalog generated by using the deep Subaru/Suprime-cam field which covers one-third of the performance verification field, and the  $g'r'i'z'$  catalog based on observations made with MegaCam at CFHT. We found  $B - R$  and  $R - z'$  colours

of sources with successful optical identifications are systematically redder than that of the entire optical sample in the same field. Moreover, approximately 40% of the 15  $\mu\text{m}$  sources show colours  $R - L15 > 5$ , which cannot be explained by the spectral energy distribution (SED) of normal quiescent spiral galaxies, but are consistent with SEDs of redshifted ( $z > 1$ ) starburst or ultraluminous infrared galaxies. This result indicates that the fraction of the ultraluminous infrared galaxies in our faint 15  $\mu\text{m}$  sample is much larger than that in our brighter 15  $\mu\text{m}$  sources, which is consistent with the evolving mid-infrared luminosity function derived by recent studies based on the Spitzer 24  $\mu\text{m}$  deep surveys. Based on an SED fitting technique, the nature of the faint 15  $\mu\text{m}$  sources is further discussed for a selected number of sources with available  $K_s$ -band data.

**Key words:** space vehicles: instruments — galaxies : evolution — galaxies : statistics — infrared galaxies

## 1. Introduction

Finding new populations of faint high-redshift galaxies is an important step to unveil the Cosmic star formation history of the Universe. Deep mid-infrared (especially at 15  $\mu\text{m}$ ) and far-infrared (at 90, 170  $\mu\text{m}$ ) surveys with the Infrared Space Observatory (ISO, Genzel, Cesarsky 2000, and references therein) discovered a distinct population with faint optical fluxes and large infrared luminosities ( $L_{\text{bol}} \geq 10^{11} L_{\odot}$ , Elbaz et al. 2002) at  $z \geq 0.5$ . The 15  $\mu\text{m}$  source counts obtained with the ISO surveys implied strong evolution in the galaxy population (Genzel, Cesarsky 2000, Aussel et al. 1999, Serjeant et al. 2001, Gruppioni et al. 2002, Oliver et al. 2002). Not only the source count models for mid-IR counts but also the X-ray data (Manners et al. 2004) and subsequent spectroscopic studies (Rowan-Robinson et al. 2004) confirmed that the bulk of the ISO sources were starburst galaxies not the AGNs.

The *Spitzer Space Telescope* (Werner et al. 2004) also offers excellent sensitivities in the four IRAC wavebands between 3.6 and 8.0  $\mu\text{m}$  (Fazio et al. 2004) and at MIPS 24  $\mu\text{m}$  (Rieke et al. 2004), and has revealed that the key epoch to understand the formation and evolution of massive ( $M \geq 10^{11} M_{\odot}$ ) galaxies is at  $z = 1 - 2$ : the star formation activity of massive galaxies at  $z \sim 2$  is hundred times larger than that at present (Chary 2006, Caputi et al. 2006). These ultra-luminous ( $L \geq 10^{12} L_{\odot}$ ) infrared galaxies (ULIRGs) may be the progenitors of present-day massive galaxies. In order to reveal their nature, we require complete, uniform samples of massive star forming galaxies at  $z = 1 - 2$ . Although the *Spitzer* 24  $\mu\text{m}$  deep surveys can probe galaxies at this redshift range, deep surveys at shorter mid-infrared wavelengths (10-20  $\mu\text{m}$ ,

---

\* Further information contact Hideo Matsuhara (maruma@ir.isas.jaxa.jp)

† Present address : Cybernet systems Co. Ltd., Bunkyo-ku, Tokyo 112-0012, Japan

in the gap between the IRAC 8  $\mu\text{m}$  band and the MIPS 24  $\mu\text{m}$  band) are very important to unveil the nature of them, since the strong 6.2 & 7.7  $\mu\text{m}$  PAH features prominent in the mid infrared spectra of star-forming galaxies can enter the MIPS 24  $\mu\text{m}$  passband only at  $z > 2$ . *Spitzer*/IRS (Houck et al. 2004) has imaging capability at 16  $\mu\text{m}$  via its peak-up camera, and with this camera deep 16  $\mu\text{m}$  surveys over 150 arcmin<sup>2</sup> in each of GOODS-North and GOODS-South fields have been carried out to depths of 50-85  $\mu\text{Jy}$  ( $3\sigma$ ) (Teplitz et al. 2007, Teplitz et al. 2005). However, the areal coverage is not yet comparable to the surveys at 24  $\mu\text{m}$  due to the relatively small field of view (1.2 arcmin<sup>2</sup>) of the IRS peak-up camera.

The AKARI satellite, launched on February 21, 2006 (UT), has the capability for deep mid-infrared imaging in the *Spitzer* wavelength desert between 8  $\mu\text{m}$  and 24  $\mu\text{m}$  through one of its focal plane instruments, the InfraRed Camera (IRC, Onaka et al. 2007). The IRC incorporates three infrared cameras covering nine bands between 2 & 24  $\mu\text{m}$  suitable for deep cosmological surveys. Note that due to the nature of the orbit of AKARI (Sun-synchronous), the visibility of any point on the sky is a strong function of ecliptic latitude and thus deep surveys are only possible at the ecliptic poles. The AKARI North Ecliptic Pole (NEP) survey is a major legacy of the AKARI mission consisting of a deep 0.4 square degree and shallow 6.2 square degree survey in all 9 IRC bands (Matsuhara et al. 2006). The AKARI NEP surveys, especially at 11, 15, and 18  $\mu\text{m}$ , are well matched to the *Spitzer* 24  $\mu\text{m}$  surveys (e.g., Papovich et al. 2004), sampling similar cosmological volumes and are more sensitive to high redshift star-formation activity than the shorter wavelength *Spitzer*/IRAC 8  $\mu\text{m}$  band.

In this paper we describe a selection of initial results from the deep extragalactic survey around the NEP region, focusing on the optical nature of the faint 15  $\mu\text{m}$  sources detected in the performance verification phase of the AKARI mission. The 15  $\mu\text{m}$  sample is especially unique since more than 100 sources are fainter than 100  $\mu\text{Jy}$ , a limit below that obtained with ISO. In section 2, we briefly describe the AKARI data as well as the optical data obtained with Subaru/Suprime-cam and CFHT/Megacam, and the results of identification of the optical counterparts. In section 3, we discuss the nature of the 15  $\mu\text{m}$  sample based on the optical – mid infrared colours. Section 4 gives the summary of the paper. Throughout the paper we use the AB magnitude system, unless otherwise explicitly noted : 20 AB mag corresponds to 36 $\mu\text{Jy}$ . We adopt a cosmology of  $\Omega_m = 0.3$ ,  $\Omega_\Lambda = 0.7$ , and  $H_0 = 70\text{km sec}^{-1} \text{Mpc}^{-1}$ .

## 2. The data and the Results of Identification

### 2.1. AKARI/IRC mid-infrared data

The NEP Deep survey is centred on a circle at R.A. = 17<sup>h</sup>55<sup>m</sup>24<sup>s</sup>, dec = +66°37'32". However, during the performance verification phase (13th April – 8th May 2006) of the AKARI mission a pilot survey of the NEP over a single field of view of the IRC (approximately 10' × 10', (hereafter referred to as the performance verification field) at R.A. = 17<sup>h</sup>57.<sup>m</sup>3, dec =

+66°54.'3), ten pointings deep in the IRC L15 band (i.e. in the 15 $\mu$ m band) was carried out.

Here we briefly report the observations and the data reduction: full details are described in Wada et al. (2007a). The data for this work were taken using the IRC05 Astronomical Observation Template (AOT) mode which is optimized for deep survey observations. Note that the IRC05 AOT minimizes overheads by using the minimum number of resets, no filter change and moreover no dithering operation during the 10 minute integration time for one pointing. Therefore, the dithering is performed among the individual pointing observations to remove the effects of dead/hot pixels and cosmic rays, etc. The total net exposure time of the ten pointing observations was 4417 seconds. The data from individual frames for each pointing were reduced using the standard IRC data reduction pipeline version 060801 (Ita, Pearson 2007) within the IRAF environment <sup>1</sup>. The IRC pipeline splits pointings into individual frames and corrects for instrument characteristics by masking of anomalous/dead pixels, and then applies dark subtraction, linearity correction, saturation, distortion correction and flat fielding, etc. Astrometric data (world coordinate system, WCS) is applied by matching bright stars within the data with 2MASS counterparts. Identification of bright point sources in the deep optical image (Wada et al. 2007b, see section 2.2) by eye suggests that the positional accuracy of the WCS is much better than two pixels (5 arcsec). The resulting stacked images for the individual pointing observations are then co-added by identifying the relatively bright sources in each processed image of one pointing. Finally the edge of the image, where the signal-to-noise ratio is worse, was trimmed, resulting in a final image size of 77.29 arcmin<sup>2</sup>. We used SExtractor (Bertin, Arnouts 1996) for the source detection, and source fluxes were evaluated by aperture photometry with a radius of 1.3 arcsec. In total 257 sources were extracted between  $L15=16$  and 20 magnitudes, of which 110 sources were fainter than 19 mag.

At present, the depth of the final L15 image is approximately 42  $\mu$ Jy in  $3\sigma$ , probably due to the fact that the source extraction technique is not yet optimized. The completeness analysis result implies that the number of sources below 150  $\mu$ Jy is substantially underestimated, but once detected, the source detection is reliable down to  $L15=20$  mag (or 36  $\mu$ Jy; Wada et al. 2007a). This is justified since 60–80% of the sources fainter than  $L15=18$  mag can be identified in the optical images (see section 2.3).

## 2.2. Optical Data

Approximately one third of the performance verification field is covered by a single Subaru Suprime-cam field of view (916 arcmin<sup>2</sup>) to  $B=28.4$ ,  $V=27$ ,  $R=27.4$ ,  $i'=27$ ,  $z'=26.2$  ( $3\sigma$ , AB magnitude, Wada et al. 2007b, in preparation). The observations were carried out in June and September 2003 with a typical seeing of 1.0 arcsec.

---

<sup>1</sup> IRAF is distributed by the National Optical Astronomy Observatory, which is operated by the Association of Universities for Research in Astronomy, Inc., under cooperative agreement with the National Science Foundation.

The remaining two thirds of the performance verification field is covered by  $g'$ ,  $r'$ ,  $i'$ ,  $z'$ -band images taken with the MegaCam instrument on the Canada-France-Hawaii Telescope (CFHT). The MegaCam observation was carried out in August/September 2004 to support the AKARI NEP survey. The observed field covers roughly a  $2^\circ$  by  $1^\circ$  field of view centered on the NEP, therefore the whole performance verification field is covered by the CFHT imaging data. The depth of the CFHT image is estimated to be  $g' \sim 26.4$  mag,  $r' \sim 25.9$  mag,  $i' \sim 25.3$  mag, and  $z' \sim 24.0$  mag at  $3\sigma$  over an aperture with  $1''.0$  diameter, but effectively the source counts are complete only down to a limit of about 1.5 magnitudes brighter than the above numbers. The absolute astrometric accuracy of the CFHT mosaic data is measured to be about r.m.s  $\sim 0''.4$ . More details on the CFHT images can be found in Hwang et al. (2007).

### 2.3. Identification with Subaru/Suprime-cam source catalog

The result of the identification within a 2 arcsec search radius is shown in Table 1. Due to the partial coverage of the Subaru image, only 105 sources are inside the Subaru image. Between  $L15=16$  and 18 magnitudes, all the three L15 sources without optical matches are found to be a blend of several sources or a part of a large, bright galaxy. Blend of several sources in L15 causes the coordinate to be calculated as the mean of the multiple sources, making it escape from the 2 arcsec matching radius. Between  $L15=18$  and 19 magnitudes, six out of seven L15 sources without optical matches are found to be a part of a bright optical counterpart, or located near the edge, or a blend of multiple sources. The remaining source is found near the edge of the L15 image. It could be a genuine mid-infrared source with no optical counterpart, but it is located near the edge of the L15 image where the signal-to-noise ratio is low. Between  $L15=19$  and 20 magnitudes, 12 sources out of 15 with no optical counterpart are again, blend of multiple sources, inside optically bright galaxies, or probably spurious objects near the edge of the L15 image. The remaining three L15 sources may be genuine optically faint sources. Overall, of 24 L15 sources without optical matches, only three or four are found to be sources without optical counterparts which are worth to be investigated carefully by multi-colour images taken during the NEP survey program. The rest are L15 detection of multiple sources, sources within optically bright galaxies, or erroneous matches near the edges.

Figure 1 shows their  $R - L15$  colour with  $15\ \mu\text{m}$  magnitude. Except for the very blue sources which are found to be bright stars (point-like sources in the Subaru image), the  $R - L15$  colour distribution does not change with  $15\ \mu\text{m}$  magnitude and has a median value of  $R - L15=4.6$  mag.

As examples showing their optical colour characteristics, in Figure 2, 3 we show a comparison of the  $B - R$ ,  $R - z'$  colours between all the Subaru sources in the NEP performance verification field and the  $15\ \mu\text{m}$  sources. The optical colours of the  $15\ \mu\text{m}$  sources show a clear trend towards a redder colour : 0.3-0.4 mag redder in  $B - R$ , and 0.2-0.5 mag in  $R - z'$ . This indicates that the  $15\ \mu\text{m}$  sources sample either a relatively high-redshift population or a popu-

**Table 1.** Summary of Identification in the Subaru Image (2 arcsec search radius)

15 $\mu\text{m}$ magnitude	No. of total 15 $\mu\text{m}$ sources	No. of sources inside the Subaru image	No. of sources with successful identification
16–18	44	18	15(0) <sup>#</sup>
18–19	103	40	33(2)
19–20	110	47	32(7)

<sup>#</sup> All 18 sources have counterparts within 3 arcsec search radius.

Numbers in the parenthesis are those with two or more optical counterparts.

**Table 2.** Summary of Identification in the CFHT Image

15 $\mu\text{m}$ magnitude	No. of sources inside the CFHT image	No. of sources in 3 arcsec search radius	No. of sources in 2 arcsec search radius
16–18	42	39(13)	27(3)
18–19	99	61(10)	50(5)
19–20	108	67(7)	49(4)

Numbers in the parenthesis are those with two or more optical counterparts.

lation exhibiting dust reddening. Moreover, the fainter 15  $\mu\text{m}$  sources at or below 18 mag(AB) show redder  $R - z'$  colour (approximately 0.3 mag) than the brighter sources. This may indicate that fainter 15  $\mu\text{m}$  sources are at relatively high redshift, since the shift of their Balmer/4000Å spectral break in between the  $R$  and  $z'$  bands will create redder  $R - z'$  colours.

#### 2.4. Identification with CFHT/Megacam source catalog

The result of the cross-identification with 2'' search radius for optical sources in the CFHT images is shown in Table 2.

We find optical counterparts for 93% of the bright L15 sources ( $16 < L15 < 18$  mag), which is consistent with the matching result using the Subaru data. A large fraction of sources with a positional offset between 2'' and 3'' turn out to be multiple optical sources blended into a single object in the L15 image. For the fainter L15 sources, the matching probability drops to  $\sim 65\%$  with a 3'' matching radius and down to 50% when we use a 2'' matching radius. The above number is about 10-30 % less than the matching probability of 60 – 80 % for L15 sources in the Subaru image. The discrepancy mainly comes from the fact that about 10% of L15 sources have optical magnitudes around  $R \sim 26$  (Figure 1) for which no  $r'$ -band counterparts are found in the CFHT image. Thus, although the CFHT image covers the entire performance verification field, we only use the sources in the Subaru image for the discussion of the nature of the faint 15  $\mu\text{m}$  sources.

One should note that the simple automatic identification presented here also suffers from

the chance coincidence. Based on the number counts of  $r'$ -band sources presented in Hwang et al. (2007), the chance coincidence of source identification is 6% and 15% for  $3''$  search radius for sources at  $r' < 22$  and  $r' < 24$ , respectively. This number drops to 3% and 7% for a  $2''$  search radius. Clearly, the  $2''$  search radius suffers much less from chance coincidence. However, a  $2''$  radius may be too small in the case for some  $15 \mu\text{m}$  sources where the mid-infrared flux originates from multiple sources.

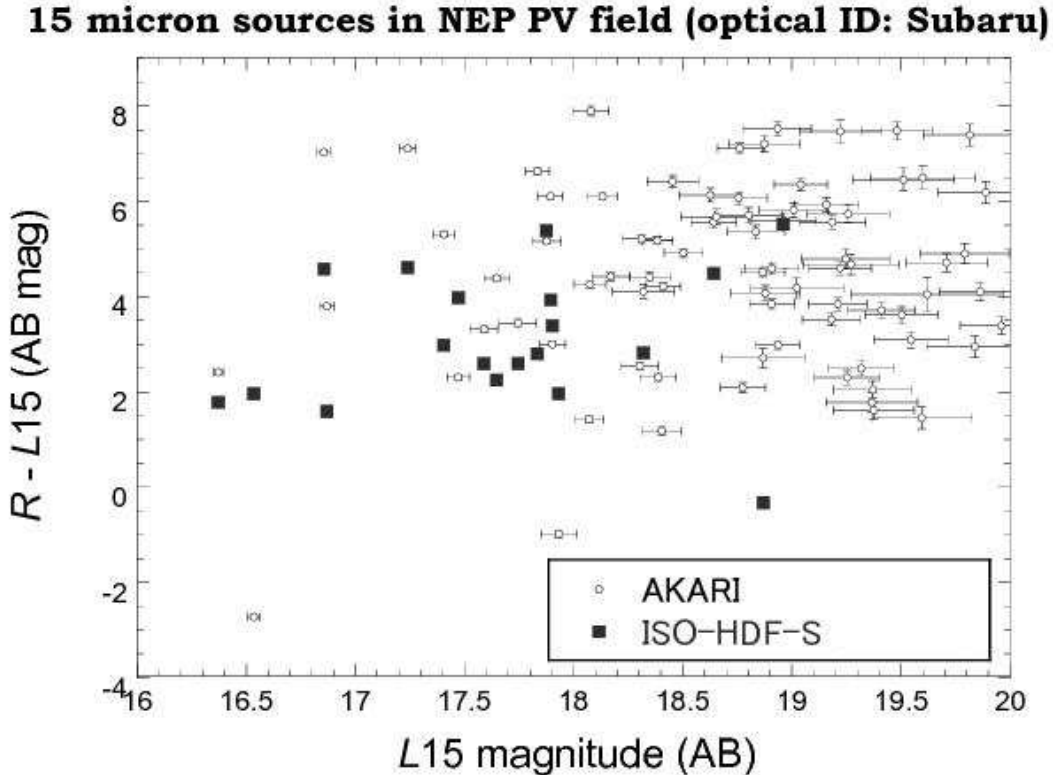


**Fig. 1.** The observed optical – mid-infrared color vs  $15 \mu\text{m}$  magnitude(AB) for all the  $15 \mu\text{m}$  sources with successful identification on the Subaru/Suprime-cam source catalog. Black squares represent the HDF-S sources detected with the ISOCAM LW3  $15 \mu\text{m}$  deep survey (Oliver et al. 2002, Mann et al. 2002).

### 2.5. Identification with KPNO/Flamingos near-infrared source catalog

The Subaru/Suprime-cam field around the NEP is also covered by the KPNO 2.1m/FLAMINGOS at  $J$ - and  $K_s$ -band to a depth of  $J=21.6$  and  $K_s=19.9$  ( $3\sigma$ ) in Vega magnitudes (“Field-NE” in Imai et al. 2007). Thus we also searched for near infrared counterparts of the  $15 \mu\text{m}$  sources with optical identifications in the Subaru/Suprime-cam images. However, the performance verification field is located at the edge of the survey field and thus the number of available images for stacking varies within the image, and also additionally suffers from image distortion from the FLAMINGOS camera. As a result, among the total 81 sources in Table 1, only 27 and 28 sources are identified in the  $J$ - and  $K_s$  bands

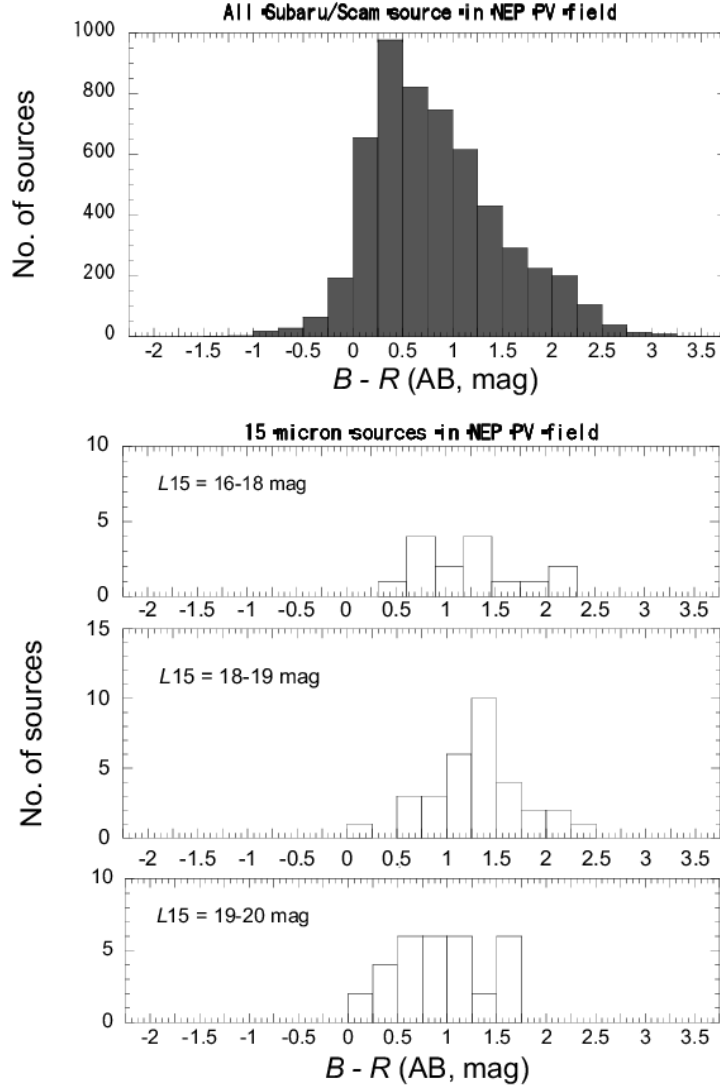


**Fig. 2.** The observed optical ( $B - R$ ) color for all  $z'$ -band selected Subaru/Suprime-cam source catalog in the field (top) and for the 15  $\mu\text{m}$  sources with successful identification on the Subaru/Suprime-cam source catalog (bottom).



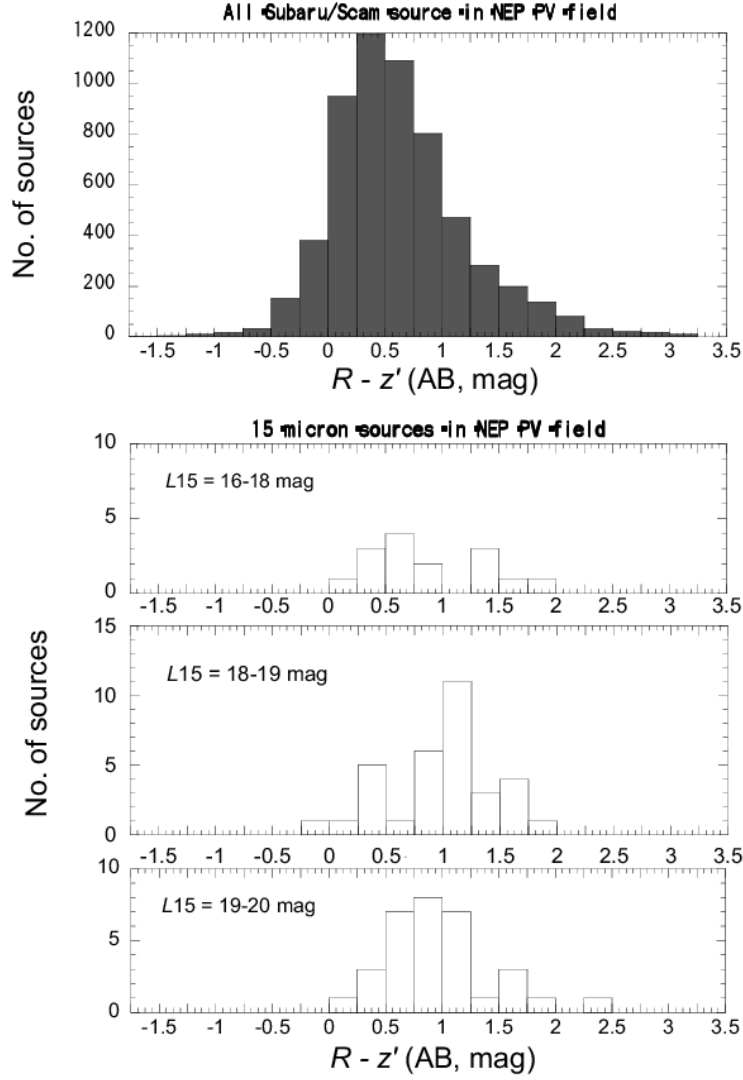


**Fig. 3.** The observed optical ( $R - z'$ ) color for all  $z'$ -band selected Subaru/Suprime-cam source catalog in the field (top) and for the 15  $\mu\text{m}$  sources with successful identification on the Subaru/Suprime-cam source catalog(bottom).

respectively, with 23 sources being identified in both the  $J$ - and  $K_s$  bands. Since the near infrared data is incomplete, we only utilize the near infrared magnitudes for the investigation of several selected sources with relatively reliable identifications (see section 3.2).

### 3. Discussion

#### 3.1. Colours of the AKARI $15\mu\text{m}$ population

In Figure 4 we plot the  $B - R$  vs  $R - L15$  colours of the AKARI  $15\mu\text{m}$  sources with successful identifications in the Subaru/Suprime-cam source catalog. The AKARI  $15\mu\text{m}$  population are plotted over 3 magnitude ranges ( $15\mu\text{m}$  AB) from 16-18, 18-19 & 19-20th magnitude. The AKARI population spans a broad range in  $R - L15$  colours from  $R - L15=1$  to 8. To investigate the colours of the AKARI  $15\mu\text{m}$  population we introduce a set of archetypal galaxy spectral energy distribution (SED) templates. These templates are shown in Figure 5 and comprise a normal quiescent spiral galaxy modeled on the SED of M51, a dusty star-forming galaxy modeled on the SED of M82, and ULIRGs modeled on the SEDs of Arp220 and HR10. The normal galaxy template is taken from the radiative transfer models of Efstathiou, Rowan-Robinson (2003) and the star-forming galaxy and ULIRG (Arp220) templates are taken from the radiative transfer models of Efstathiou et al. (2000). We also include another ULIRG template modeled on the SED of HR10 (Graham, Dey 1996) using the starburst spectral template library of Takagi et al. (2003a, 2003b). HR10 at  $z=1.44$  is one of famous Extremely Red Objects (EROs) and its best-fitting SED model is characterized by an older age and larger stellar mass than those of Arp220 (Takagi et al. 2003b). In Figure 6 we plot the  $R - L15$  color of our model templates smoothed by the AKARI IRC filter-band response curves as a function of redshift. In general for any redshift, the dusty infrared sources are well separated from the normal quiescent galaxies, consistently having  $R - L15 > 4$ . Figure 6 also suggests that sources with  $R - L15 > 6$  or 7 may be plausible candidates for redder dusty star-forming galaxies and ULIRGs respectively at  $1 < z < 2$ . Since at  $z=1-2$  the PAH emission features at  $6.2$  and  $7.7 \mu\text{m}$  from the star-forming galaxies enter the L15 passband and thus  $R - L15$  colour becomes redder, these red  $R - L15$  colours may provide useful selection methods for high redshift ULIRGs. The  $B - R$  vs  $R - L15$  colours plotted in Figure 4 show that there is indeed a significant redder population of AKARI sources with  $R - L15 > 4$  that cannot be explained by the colours of normal quiescent galaxies or low-redshift star-forming galaxies. For these sources with  $15\mu\text{m}$  AB magnitudes of 18, 19, this correspond to  $R$  magnitudes of  $>22$ ,  $>23$  respectively.

For the AKARI  $15\mu\text{m}$  sources with successful identifications in the Subaru/Suprime-cam source catalog we find approximately 60 (40) per cent of the population with  $R - L15 > 4$  (5). There is also a significant fraction of the population (25 per cent) with very red colours of  $R - L15 > 6$ . It is noteworthy that the sources detected in the ISOCAM deep surveys in the HDF-S (Oliver et al. 2002, Mann et al. 2002) show mostly bluer ( $R - L15 < 5$ ) colours

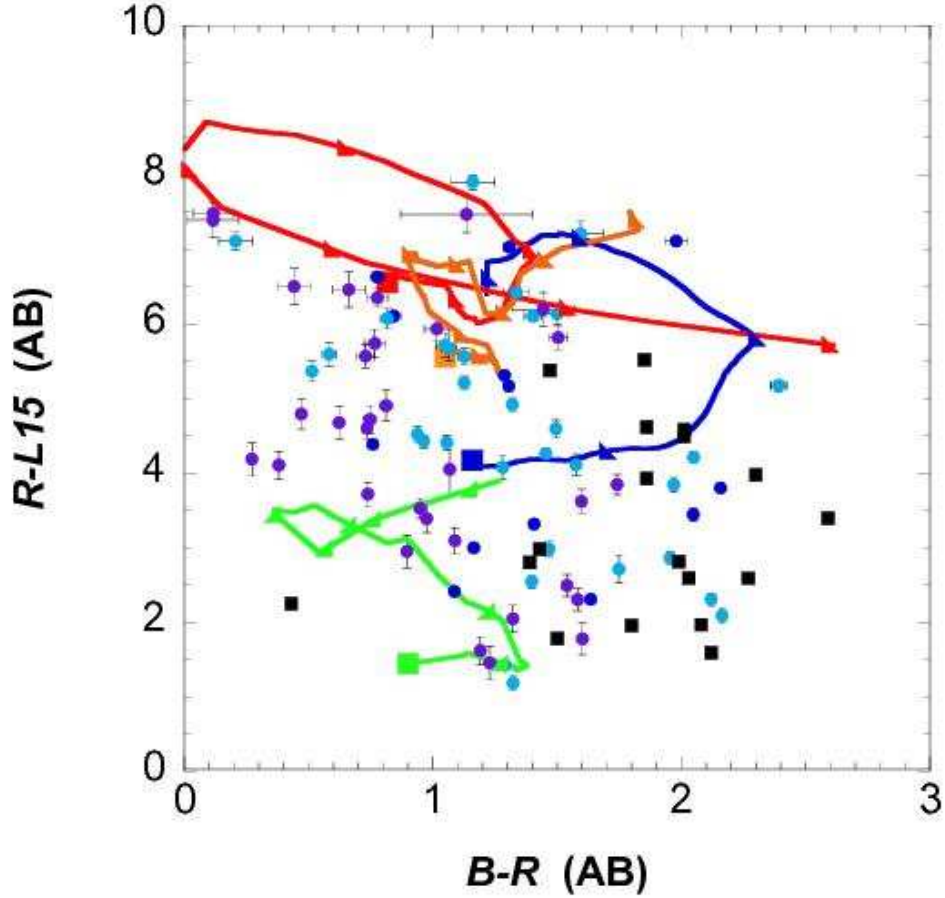


**Fig. 4.**  $B - R$  vs  $R - L15$  plot for the  $15 \mu\text{m}$  sources with successful identifications in the Subaru/Suprime-cam source catalog. Dark-blue, light-blue, & purple, circles represent 16-18, 18-19, 19-20 AKARI  $15\mu\text{m}$  AB magnitudes respectively. Color-color tracks for 4 SED templates are presented. Black squares represent the HDF-S sources detected with the ISOCAM LW3 deep survey (Oliver et al. 2002, Mann et al. 2002). Green: a normal quiescent spiral galaxy (M51 template), blue: a star-forming galaxy (M82 template), red: an Ultraluminous infrared galaxy (ULIRG) Arp220 template, orange: an ULIRG, HR10 template. The large coloured squares are the zero redshift points for the SED templates and the markers along the template color tracks represents steps of 0.5 in redshift.

except for two sources, perhaps due to its shallower depth. These red sources populate the colour-colour parameter space occupied by the model SED templates for high redshift ULIRGs in Figure 4. Note that Rowan-Robinson et al. (2004) found that around  $\sim 14$  per cent of the sources in the ELAIS final band merged catalogue ( $S_{15\mu m} > 0.7\text{mJy}$ ) could be attributed to ULIRGs. Given the deeper nature of the AKARI NEP survey, we may expect a significantly larger fraction of ULIRGs in our sample that most probably populate the  $R - L15 > 6$  region of the  $B - R$  vs  $R - L15$  colour-colour plane. This interpretation is also supported by the evolving mid-infrared luminosity function recently derived based on the Spitzer 24  $\mu\text{m}$  deep surveys (Le Floc'h et al. 2005, Pérez-González et al. 2006). Although we do not show the track for the AGN template SED, it should be noted that the power-law SEDs of dusty obscured AGN can satisfy  $R - L15 > 5$  for the power-law index  $\alpha < -1.5$  ( $f_\nu \propto \nu^\alpha$ ). Alonso-Herrero et al. (2005) present a sample of such AGN SEDs from  $\alpha = -0.5$  down to  $\alpha = -2.8$ . Thus, it is likely that a fraction of our  $15\mu\text{m}$  sources may in fact be highly obscured AGN.

So far the spectroscopic redshifts for the red  $15\mu\text{m}$  sources are not available, and it is not easy to estimate their physical quantities, such as infrared luminosities, and stellar masses. However, for near-future follow-up studies, it is valuable to present a crude picture of the sources via optical colours. Figure 7 shows a  $B - R$  vs  $R - z'$  plot for the  $15\mu\text{m}$  sources with  $R - L15 > 5$ , compared with the SED templates of the starburst (M82), ULIRGs (Arp220, HR10). The red  $15\mu\text{m}$  sources are distributed widely over the colour parameter space, but at least we can say that the colours can be explained by the SED templates with  $z \leq 2$ . Of course the SED templates presented here are not unique and there exists a wide variety of SED shapes for starburst galaxies (see also Takagi et al. in this volume). Thus optical and near infrared spectroscopic follow-ups with ground-based telescopes are essential to understand the nature of these red  $15\mu\text{m}$  sources.

### 3.2. Nature of the Selected $15\mu\text{m}$ Sources

If the  $15\mu\text{m}$  sources are located at  $z \geq 1$ , quantitative studies of the  $15\mu\text{m}$  sources require near infrared ( $J$  &  $K_s$ -band) photometry, since the Balmer or 4000Å break of the galaxy's SED is redshifted beyond optical wavelengths. For example, we may classify the  $15\mu\text{m}$  sources into either Extremely Red Objects (Mannucci et al. 2002, Miyazaki et al. 2003) or BzKs (Daddi et al. 2004) based on their colour - colour criteria. Unfortunately the  $K_s$ -band data available so far is found to be too shallow to extract the BzK population at high redshift ( $1.4 < z < 2.5$ , Daddi et al. 2004). However we found six sources satisfying the ERO criterion ( $R - K_s > 3$  in AB magnitude), and thus we attempt SED fitting of these sources in order to estimate their photometric redshifts, infrared luminosities, and SED types.

We fitted the observed SEDs using the Bayesian photometric redshift code of Benítez (2000). For the SED templates to compare with the data, we adopted 100 SEDs of IR luminous galaxies from Chary, Elbaz (2001). These SEDs are modified by applying

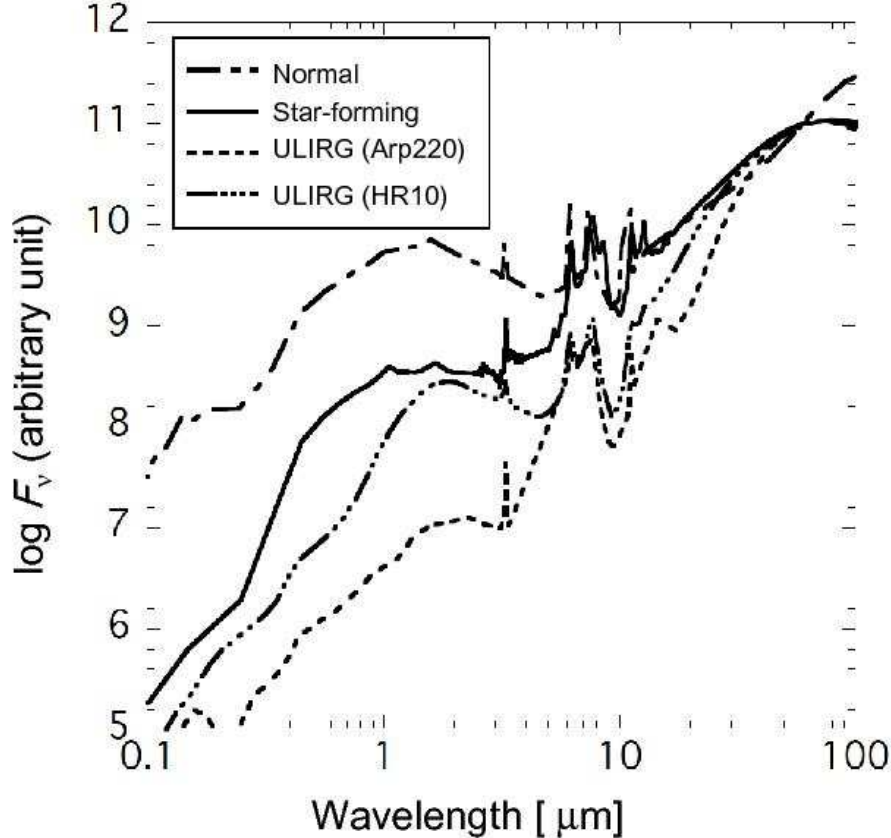


**Fig. 5.** Rest-frame optical to far-infrared spectral energy distribution templates for; dashed line: a normal quiescent spiral galaxy (M51 template), solid line: a star-forming galaxy (M82 template), dotted line: an ultraluminous infrared galaxy (ULIRG), Arp220 template, dash-dash-dot-dot: an ULIRG, HR10 template. Model templates are taken from Efstathiou, Rowan-Robinson (2003) for the normal galaxy template, Efstathiou et al. (2000) for the star-forming and Arp220 templates and Takagi et al. (2003b) for the HR10 template.

Galactic extinction corrections of  $E(B - V) = 0.041$  estimated from the far-infrared brightness of the NEP (Schlegel et al. 1998) using the extinction curve of Calzetti et al. (2000). After fitting, we obtain an estimate of the photometric redshift as well as the best-fit SED template. The infrared luminosity is calculated by integrating the fluxes beyond the rest-frame  $5 \mu\text{m}$  of the best-fit SED template. We find that the formal errors in the photometric redshifts from the fitting program are under 20%, and the uncertainty in the IR luminosity to be of order of at least a factor of a few. The estimates, however, might have a larger uncertainty if an object has a more complex SED than a simple, single-component SED as demonstrated for the object ID151 described below. We expect these uncertainties will be reduced when we have data between the  $J$ -band and the  $15 \mu\text{m}$ , and also at  $24 \mu\text{m}$  at the end of the NEP survey.

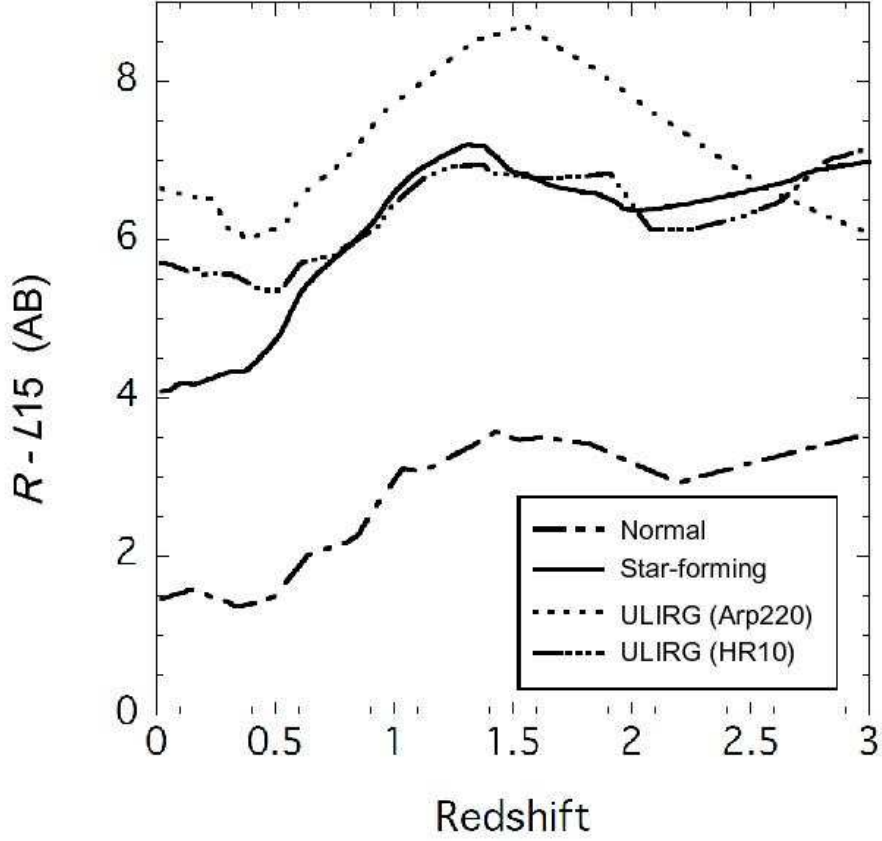


**Fig. 6.** Optical to mid-infrared ( $R - L15$  colour vs redshift for various template SEDs shown in Figure 5. The SEDs are convolved with the filter-band response curves and then the colour is derived.

### 3.2.1. Dusty Starburst Candidates

Among the six  $15 \mu\text{m}$  sources satisfying the ERO criterion, two sources (ID131 and ID52) can be fitted well with  $z \sim 1$  dusty starburst templates. In Figure 8 and 9, the results are shown: for ID131, the SED fitting gives a photometric redshift ( $z_{\text{phot}}$ ) of  $1.06 \pm 0.14$ , and total infrared luminosity ( $L_{\text{IR}}$ ) of  $1.1 \times 10^{12} L_{\odot}$ , while for ID52,  $z_{\text{phot}} = 0.97 \pm 0.13$ ,  $L_{\text{IR}} = 2.4 \times 10^{12} L_{\odot}$ .

### 3.2.2. E/S0 plus Dusty Starburst Composites?

The optical –  $K_s$ -band SEDs of the final four  $15 \mu\text{m}$  sources satisfying the ERO criterion can be fitted well by not only the dusty starburst templates at  $z=0.47$  (Figure 10 top) but also by old E/S0 like SEDs. However, for the latter case the  $15 \mu\text{m}$  fluxes originating from the circumstellar dust of the AGB stars seems to be too weak to explain the observed fluxes. Therefore we propose that the SEDs can be explained by a composite SED of the E/S0-like stellar population plus the dusty starburst population. As shown in Figure 10 middle, the SED of ID151 can be fitted by 0.8 Gyr-old (after a burst of star-formation over 0.1 Gyr produced by the 1996 version of Bruzual, Charlot (1993) models) stellar population and a dusty

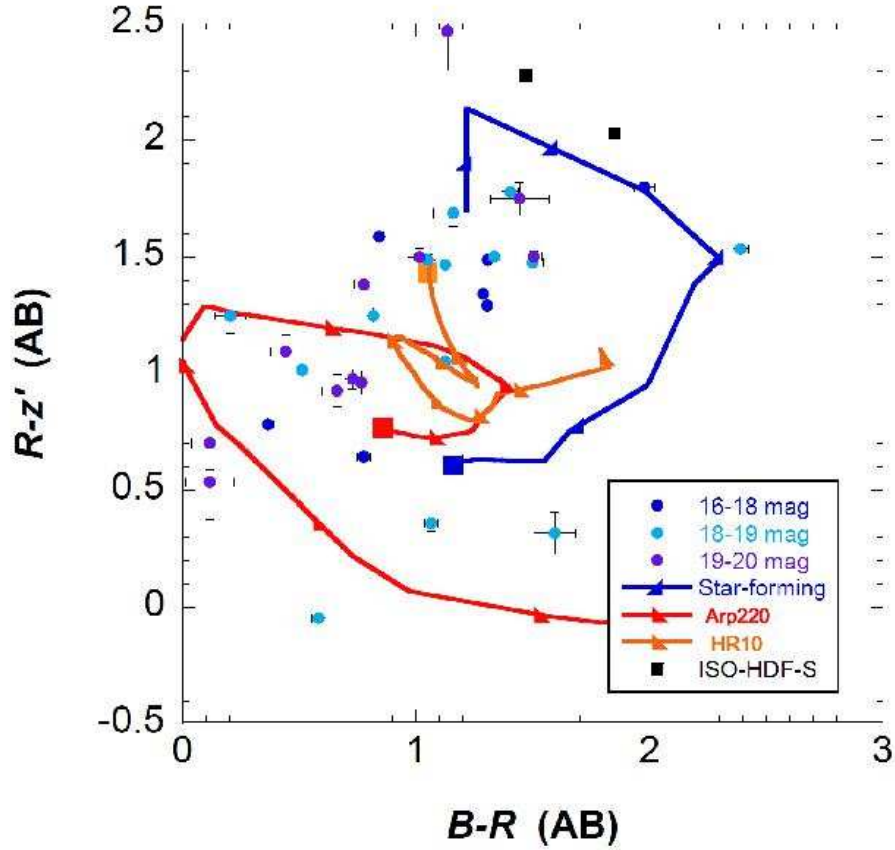


**Fig. 7.**  $B - R$  vs  $R - z'$  plot for the  $15 \mu\text{m}$  sources with  $R - L15 > 5$  in the Subaru/Suprime-cam source catalog. Dark-blue, light-blue, & purple, circles represent 16-18, 18-19, 19-20 AKARI  $15\mu\text{m}$  AB magnitudes respectively. Two black squares represent the HDF-S sources (Oliver et al. 2002, Mann et al. 2002). Color-color tracks for 3 SED templates are presented: blue: a star-forming galaxy (M82 template), red: an ultraluminous infrared galaxy (ULIRG), Arp220 template, orange: an ULIRG, HR10 template. The large coloured squares are the zero redshift points for the SED templates and the markers along the template color tracks represents steps of 0.5 in redshift.

starburst with  $L_{\text{IR}} = 10^{12} L_{\odot}$  which contributes 20% of the  $K_s$ -band flux. In this case we obtain  $z_{\text{phot}} = 1.47 \pm 0.10$ . At the moment both fits seem to be acceptable. Measurements in the intermediate bands (3-11  $\mu\text{m}$ ) soon available from the AKARI “NEP-Deep” survey will help to break this degeneracy.

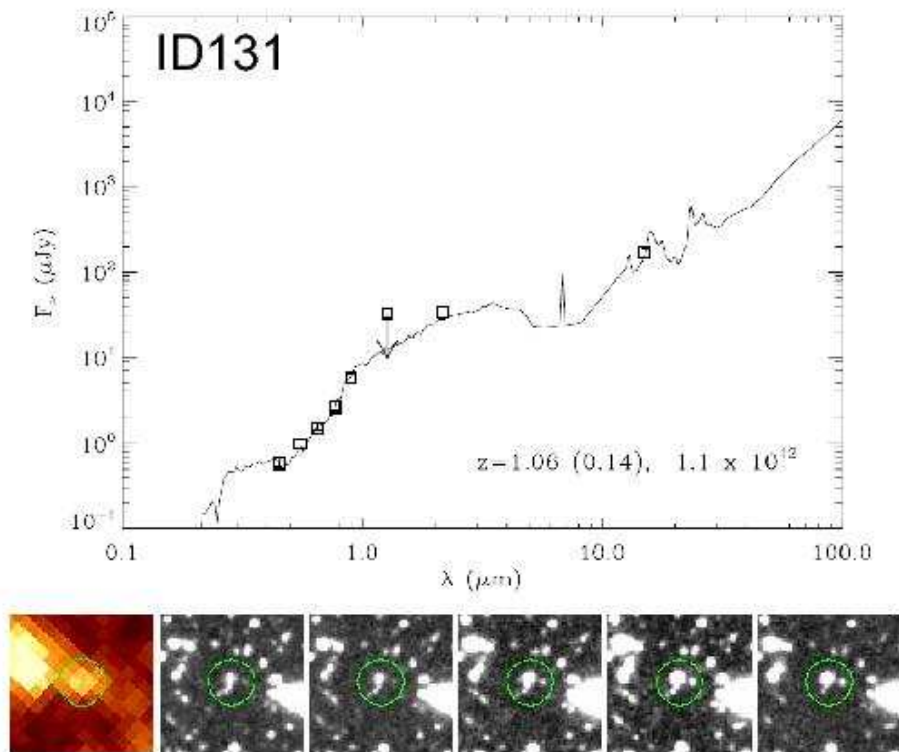


**Fig. 8.** An example of the SED fitting (top) and the postage stamp images (bottom,  $L15$ ,  $B$ ,  $V$ ,  $R$ ,  $i'$ , and  $z'$  from left to right) for sources with secure  $K_s$  photometric data, in case of ID131. The radius of circles in all the postage stamps is 5 arcsec.

The AKARI NEP survey (Matsuhara et al. 2006) is continuing and will achieve comparable mid-infrared depths to those described in this paper, over nine bands between 2 and 24  $\mu\text{m}$ . Since the “NEP-Deep” field covers approximately 20 times larger area than the performance verification field, we can expect to discover about 2000 faint ( $\leq 100 \mu\text{Jy}$ ) sources, from which we can construct statistically meaningful, optical – mid infrared SED samples to further understand the nature of the 15  $\mu\text{m}$  population introduced in this paper.

#### 4. Summary

The results of optical identifications are presented for 257 15  $\mu\text{m}$  sources detected with a deep 15  $\mu\text{m}$  survey over approximately 80 arcmin<sup>2</sup> area in the AKARI performance verification field around the North Ecliptic Pole. In comparison with the previous 15  $\mu\text{m}$  surveys with



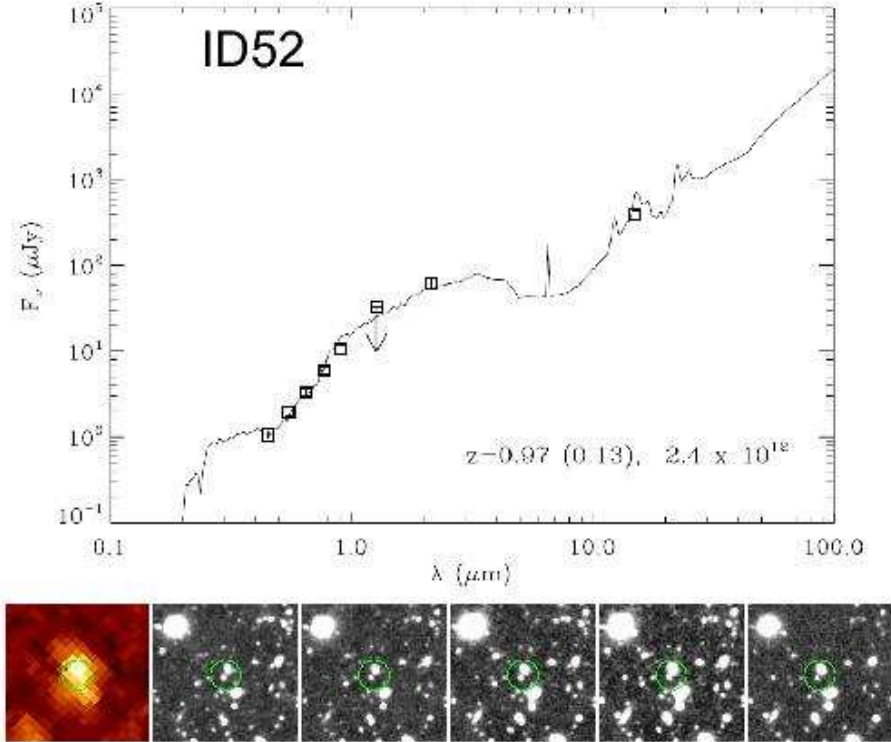


**Fig. 9.** An example of the SED fitting (top) and the postage stamp images (bottom), in case of ID52. See Figure 8 caption for explanation of figures.

ISO/ISOCAM and the *Spitzer*/IRS peak-up imaging, the AKARI 15  $\mu\text{m}$  sample is particularly unique in its faint flux limit ( $\sim 40 \mu\text{Jy}$ ): the 15  $\mu\text{m}$  fluxes of approximately a half of the sample are below 100  $\mu\text{Jy}$ . Optical counterparts were searched for within a 2-3 arcsec search radius in both a  $BVRiz'$  catalog generated from the deep Subaru/Suprime-cam field which covers one-third of the performance verification field, and the  $g'r'i'z'$  catalog based on a wide-area survey made with MegaCam at CFHT. We found that the  $B-R$  and  $R-z'$  colours of sources with successful optical identifications are systematically redder than that of the entire optical sample in the same field, indicating that the 15  $\mu\text{m}$  sources may be located at relatively high redshift. Moreover, approximately 40% of the 15  $\mu\text{m}$  sources show colours  $R-L15 > 5$ , which cannot be explained by the SED of normal quiescent spiral galaxies, but is consistent with the SEDs of redshifted ( $z > 1$ ) starburst or ULIRGs. This result indicates that the fraction of the ULIRGs in the faint 15  $\mu\text{m}$  sample is much larger than that in the brighter 15  $\mu\text{m}$  sample. Based on optical to 15  $\mu\text{m}$  SED fitting for a few sources with the  $K_s$ -band data available so far, we found that several 15  $\mu\text{m}$  sources can be explained by an SED of the dusty starburst population (ULIRGs). Deep  $J$  &  $K_s$ -band data as well as AKARI mid-infrared multi-band data other than 15  $\mu\text{m}$  are essential to further constrain the nature of the faint 15  $\mu\text{m}$  population.

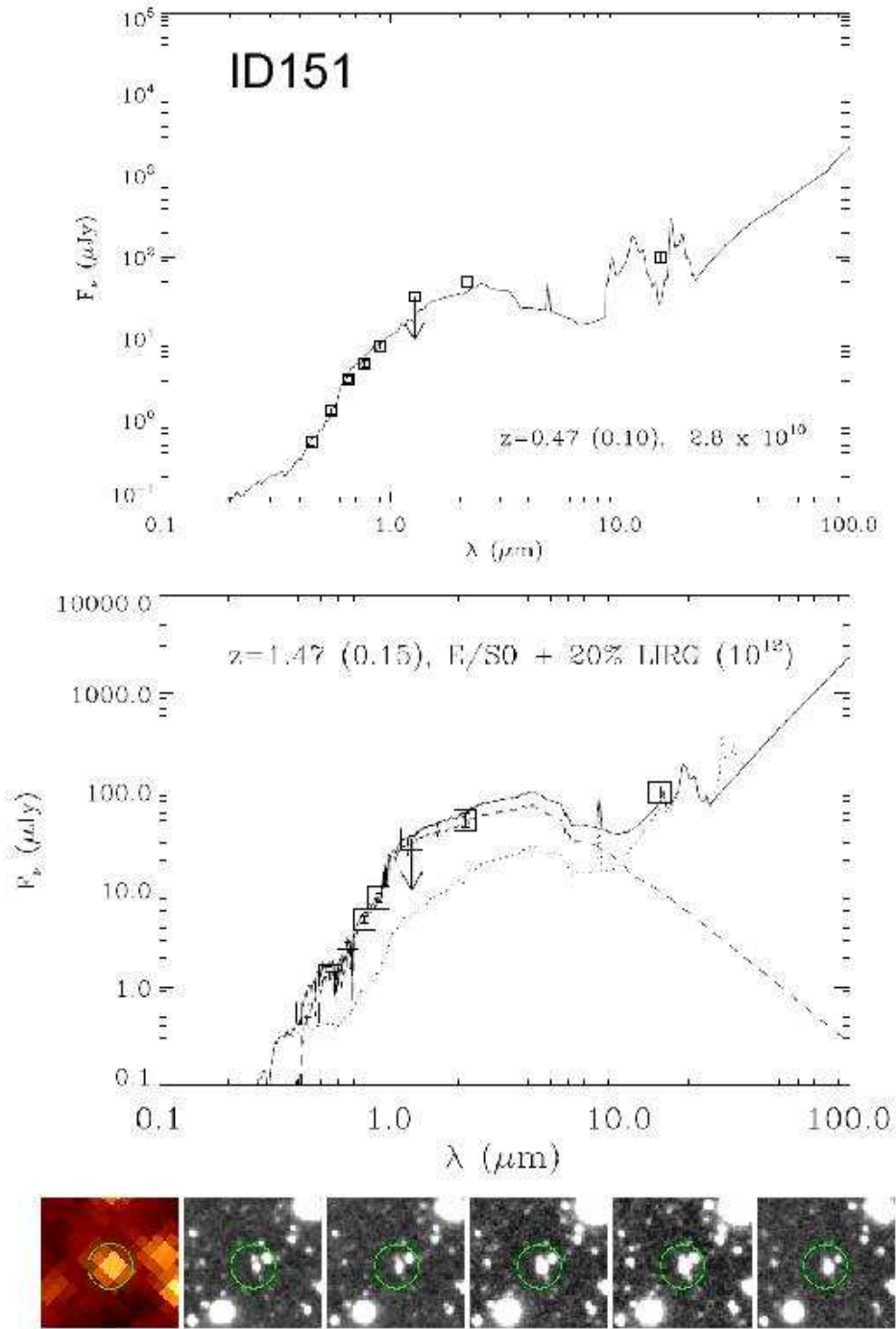


**Fig. 10.** An example of the SED fitting (top two panels) and the postage stamp images (bottom) for the sources which can be fitted with not only by the dusty starburst templates but also by composites of E/S0 and dusty starburst SEDs. See Figure 8 caption for explanation of figures.

## Acknowledgements

This work is based on observations with AKARI, a JAXA project with the participation of ESA. We would like to thank all AKARI team members for their support on this project. M.I. and E.K. were supported by the Korea Science and Engineering Foundation (KOSEF) grant funded by the Korea government (MOST), No. R01-2005-000-10610-0. H.M.L and M.G.L. were supported in part by ABRL (R14-2002-058-01000-0). This work is partly supported by the JSPS grants (grant number 15204013, and 16204013).

## References

- Aussel et al. 1999, *A&A*, 342, 313  
Alonso-Herrero, A. et al. 2006, *ApJ*, 640, 167  
Benítez, N. 2000, *ApJ*, 536, 571  
Bertin, E., Arnouts, S. 1996, *A&AS*, 117, 393  
Bruzual, A. G., Charlot, S. 1993, *ApJ*, 405, 538  
Calzetti, D., Armus, L., Bohlin, R.C., Kinney, A.L., Koornneef, J., Storchi-Bergmann, T. 2000, *ApJ*, 533, 682  
Caputi, K.I., Dole, H., Lagache, G., McLure, R.J., Puget, J.-L., Rieke, G. H., Dunlop, J.S., Le Floc'h, E., Papovich, C., Pérez-González, P.G. 2006, *ApJ*, 637, 727  
Chary R. 2006, in proceedings of “At the Edge of the Universe” conference, Sintra, Portugal, Oct. 2006 (arXiv:astro-ph/0612736v1)  
Chary, R., Elbaz, D. 2001, *ApJ*, 556, 562  
Daddi, E., Cimatti, A., Renzini, A., Fontana, A., Mignoli, M., Pozzetti, L., Tozzi, P., Zamorani, G. 2004, *ApJ*, 617, 746 (astro-ph/0409041)  
Efstathiou, A., Rowan-Robinson, M., Siebenmorgen, R., 2000, *MNRAS*, 313, 734  
Efstathiou, A., Rowan-Robinson, M., 2003, *MNRAS*, 343, 322  
Elbaz, D., et al. 2002, *A&A*, 384, 848  
Fazio, G.G., et al. 2004, *ApJS*, 154, 10  
Franceschini, A., et al. 2003, *A&A*, 403, 501  
Genzel, R., Cesarsky, C. J. 2000, *ARA&A*, 38, 761  
Graham, J. R. & Dey, A., 1996, *ApJ*, 471, 720  
Grupponi, et al. 2002, *MNRAS*, 335, 831  
Houck, J. et al. 2004, *ApJS*, 154, 18  
Hwang, N. et al. 2007, *ApJS*, submitted  
Imai, K., Matsuhara, H., Oyabu, S., Wada, T., Takagi, T., Fujishiro, N., Hanami, H., & Pearson, C.P. 2007, *AJ*, in press  
Ita, Y., Pearson, C.P., 2007, *IRC Data User’s Manual*  
Le Floc’h, E. et al. 2005, *ApJ*, 632, 169  
Mann, R.G. et al. 2002, *MNRAS*, 332, 549  
Manners, et al. 2004, *MNRAS*, 355, 97

Mannucci, F., et al. 2002 MNRAS, 329, L57  
Matsuhara, H., Shibai, H., Onaka, T., & Usui, F. 2005, Advances in Space Research, 36, 1091  
Matsuhara, H. et al. 2006, PASJ, 58, 673,  
Miyazaki, M. et al. 2003, PASJ, 55, 1079  
Murakami, H. et al. 2007, PASJ, this volume  
Oliver, S. et al. 2002, MNRAS, 332, 536  
Onaka, T. et al. 2007, PASJ, this volume  
Papovich, C. et al., 2004, ApJS, 154, 70  
Pearson, C.P. 2005, MNRAS, 358, 1417  
Pérez-González, P.G. et al. 2005, ApJ, 630, 82  
Rieke, G.H., et al. 2004, ApJS, 154, 25  
Rowan-Robinson, M. et al., 2004, MNRAS, 351, 1290  
Serjeant, S. et al. 2001, MNRAS, 316, 768  
Schlegel, D.J., Finkbeiner, D.P., Davis, M. 1998, ApJ, 500, 525  
Takagi T., Arimoto N., Hanami H., 2003, MNRAS, 340, 813  
Takagi T., Vasevičius, V., Arimoto N., 2003, PASJ, 55, 385  
Teplitz, H., I. Charmandaris, V., Chary, R., Colbert, J., W., Armus, L., Weedman, D., 2005, ApJ, 634,  
128  
Teplitz, H.I., Chary, R., Colbert, J.W., Siana, B., Elbaz, D., Dickinson, M., Papovich, C. 2007,  
AAS/AAPT Joint Meeting, American Astronomical Society Meeting 209, #132.03  
Wada, T., et al. 2007, PASJ, in this volume  
Wada, T., et al. 2007, in preparation  
Werner, M.W., et al. 2004, ApJS, 154, 1